EARTH SURFACE PROCESSES AND LANDFORMS
*Earth Surf. Process. Landforms* , ()

Published online in Wiley Online Library
(wileyonlinelibrary.com) DOI: 10.1002/esp.4885

# The influence of lithology on channel geometry and bed sediment organization in mountainous hillslope-coupled streams

**Michael Mulugetta Fratkin,[1,2] Catalina Segura[1]* and Sharon Bywater-Reyes[3]**
[1] Forest Engineering, Resources, and Management, Oregon State University, Corvallis, OR USA
[2] Water Resources Graduate Program, Oregon State University, Corvallis, OR USA
[3] Department of Earth and Atmospheric Sciences, University of Northern Colorado, Greeley, CO USA

Received 4 June 2019; Revised 22 April 2020; Accepted 23 April 2020

*Correspondence to: Catalina Segura, Forest Engineering, Resources, and Management, Oregon State University, Corvallis, OR, USA. E-mail: catalina.segura@oregonstate.edu

ESPL
Earth Surface Processes and Landforms

ABSTRACT: Sediment transport and channel morphology in mountainous hillslope-coupled streams reflect a mixture of hillslope and channel processes. However, the influence of lithology on channel form and adjustment and sediment transport remains poorly understood. Patterns of channel form, grain size, and transport capacity were investigated in two gravel-bed streams with contrasting lithology (basalt and sandstone) in the Oregon Coast Range, USA, in a region in which widespread landslides and debris flows occurred in 1996. This information was used to evaluate threshold channel conditions and channel bed adjustment since 1996. Channel geometry, slope, and valley width were measured or extracted from LiDAR and sediment textures were measured in the surface and subsurface. Similar coarsening patterns in the first few kilometres of both streams indicated strong hillslope influences, but subsequent downstream fining was lithology-dependent. Despite these differences, surface grain size was strongly related to shear stress, such that the ratio of available to critical shear stress for motion of the median surface grain size at bankfull stage was around one over most of the surveyed lengths. This indicated hydraulic sorting of supplied sediment, independent of lithology. We infer a cycle of adjustment to sediment delivered during the 1996 flooding, from threshold conditions, to non-alluvial characteristics, to threshold conditions in both basins. The sandstone basin can also experience complete depletion of the gravel-size alluvium to sand size, leading to bedrock exposure because of high diminution rates. Although debris flows being more frequent in a basalt basin, this system will likely display threshold-like characteristics over a longer period, indicating that the lithologic control on channel adjustment is driven by differences in rock competence that control grain size and available gravel for bed load transport. © 2020 John Wiley & Sons, Ltd.

KEYWORDS: sediment transport capacity; threshold channel; hillslope coupled; gravel-bed river; Oregon coast range

## Introduction

Hillslope-coupled headwater streams are common in mountainous regions throughout the world and are an important source of sediment to downstream systems (Benda, 1990; Richardson *et al.*, 2002; Campbell and Church, 2003; Benda *et al.*, 2005; Reid *et al.*, 2007). In these streams, mass-wasting events such as debris flows and landslides alter channel processes by introducing large pulses of sediment (Korup, 2004; Brummer and Montgomery, 2006; Rickenmann and Koschni, 2010; Mouri *et al.*, 2011; Kuo and Brierley, 2014) and wood (Nakamura and Swanson, 1993; Jones *et al.*, 2000; Massong and Montgomery, 2000; May and Gresswell, 2003). Indeed, in mountainous first- to third-order streams, debris flows and landslides are typically the main source of sediment (Swanson *et al.*, 1982; Benda and Dunne, 1987; Wells and Harvey, 1987; Slaymaker, 1993; Brardinoni *et al.*, 2003; Benda *et al.*, 2005; Church, 2010). Further downstream, fluvial processes dominate the movement of water and sediment within alluvial and non-alluvial reaches (Montgomery and Buffington, 1997).

Alluvial streams are self-formed, carved in the sediments that they have transported and deposited (Church, 2006). In contrast, bedrock streams or streams choked with colluvium delivered from hillslopes are unable to adjust their boundaries. These streams, at least over some time (Booth and Bledsoe, 2009), do not adhere to the definition of 'alluvial' sensu Church (2006), and will therefore be referred to as 'non-alluvial' in this paper. Although the channel bed in many streams draining coupled terrain is characterized by alluvial cover dominated by cobble- and gravel-sized material, field evidence indicates that fourth- to fifth-order streams in landscapes where debris flows are important can go over cycles of degradation down to bedrock and aggradation of several metres of sediment depending on sediment supply (Benda, 1990).

Fluvial adjustments in gravel-bed alluvial rivers have been investigated for the last 50 years based on threshold channel theory (Parker, 1978, 1979), considering longitudinal variations

of channel geometry and grain size (Pizzuto, 1992; Pitlick and Cress, 2002; Torizzo and Pitlick, 2004; Eaton and Church, 2007; Parker *et al.*, 2007; Mueller and Pitlick, 2014; Eaton and Millar, 2017) in a wide range of conditions, including headwater streams (Mueller and Pitlick, 2005; Green *et al.*, 2015). The premise in these investigations — inferred indirectly from statistical relationships — is that gravel-bed rivers are adjusted to the supply of gravel with a specified grain size distribution (independent variable), and the adjustment involves modifying the channel's width, depth, and slope to achieve transport continuity with stable banks. However, studies have shown both experimentally (Dietrich *et al.*, 1989; Buffington and Montgomery, 1999; Eaton and Church, 2009; Madej *et al.*, 2009) and in the field (Mueller and Pitlick, 2013) that fluvial adjustment to changes in sediment supply can occur via channel grain size sorting. That is, the channel grain size becomes the dependent variable, while the channel size remains mainly unchanged. Threshold channels at bankfull flow have a shear stress adjusted to transport the median-size gravel particle (Parker, 1978, 1979). The applicability of threshold channel theory to gravel-bed streams influenced by hillslope processes has been limited (Brummer and Montgomery, 2003; Tranel, 2018), with a recent study arguing that rivers subject to high sediment supply, such as streams located in tectonically active settings like the Oregon Coast Range, USA, may not exhibit threshold-like conditions (Pfeiffer *et al.*, 2017).

Lithology may influence the adjustment of hillslope-coupled streams through both differential sediment supply and diminution rates. Indeed, lithology was identified as the primary control of bankfull sediment concentration — proxy for sediment supply — with higher concentrations reported for streams draining softer lithologies in a study that considered 80 streams in the Rocky Mountains, USA (Mueller and Pitlick, 2013). Lithology influences in-channel processes in alluvial rivers given variations in rock friability, which can contribute to longitudinal sediment fining through abrasion and diminution processes. These processes can ultimately influence the proportion of sediment carried as bed load or suspended load. The result in many instances is a systematic variation in sediment flux and size driven by variations in sediment supply and abrasion rates of different lithologies (Pizzuto, 1995; Attal and Lavé, 2006; Chatanantavet *et al.*, 2010; O'Connor *et al.*, 2014; Menting *et al.*, 2015; Mueller *et al.*, 2016). For example, in western Oregon (USA), sediment in rivers draining friable lithologies experiences rapid fining and reduced bed load transport rates as coarse sediment is lost to abrasion (O'Connor *et al.*, 2014). A similar effect was observed for the Henry Mountains (Utah, USA), in which streams draining more friable material had higher incision rates, more exposed bedrock, finer bed material, and lower slopes than streams draining more competent material (Johnson *et al.*, 2009). Perhaps counterintuitive, friable lithologies often result in more bedrock reaches as material is lost to abrasion and removed from the system.

Lithology may additionally influence hillslope–fluvial coupling through contrasting hillslope evolution and mass-wasting processes (Marston *et al.*, 1997; Roering *et al.*, 2005; Miller and Burnett, 2008; May *et al.*, 2013; Johnstone and Hilley, 2015; Beeson *et al.*, 2018). This in turn may influence the presence of alluvial or non-alluvial conditions and contrasting longitudinal adjustments of channel geometry and grain sizes through differential hillslope sediment inputs. For example, an investigation of debris torrents in the Oregon Coast Range indicated that they were twice as frequent in basins draining rocks with low friability (such as basalt) compared to basins draining rocks with high friability (such as sandstone) (Marston *et al.*, 1997). In addition, deep-seated landslides often found in streams draining softer lithology (sandstone) appear to be associated with wider streams as a result of long-term sediment inputs in these regions (Roering *et al.*, 2005; May *et al.*, 2013; Beeson *et al.*, 2018).

The goal of this study is to investigate the longitudinal patterns of channel form and grain size in two gravel-bed streams in the Oregon Coast range (USA) that drain contrasting lithologies (basalt vs. sandstone) in a landscape in which debris flows and landslides are common, with many triggered in the flood of record in 1996 (Swanson *et al.*, 1998; Robinson *et al.*, 1999; Johnson *et al.*, 2000; Miller and Benda, 2000; May, 2002; Faustini and Jones, 2003; Lancaster *et al.*, 2003). Few studies have investigated the longitudinal variation in channel geometry, grain size, and sediment transport capacity in the context of channel adjustment in this region, although alluvial cover has been documented in many of these streams (Marston *et al.*, 1997; Massong and Montgomery, 2000; Montgomery *et al.*, 2003; May and Gresswell, 2004; Sable and Wohl, 2006). By considering information about mass wasting, longitudinal grain-size trends, and transport capacity as a function of underlying lithology, we build a comprehensive picture of how mountainous headwater streams adjust after a large pulse of sediment supply, and the degree to which these systems conform to threshold channel theory. We expected differences in channel adjustment since the 1996 mass-wasting events between basalt and sandstone basins related to the competency of the delivered sediment. We expected that the basalt basin would display threshold channel conditions due to the high competency of basalt that would prevent the loss of alluvium to abrasion. In contrast, we expected that the sandstone basin would display non-threshold conditions with evidence for a transition to bedrock, driven by high diminution rates in this softer lithology which would result in a lack of alluvial cover.

## Study Area

We investigated two basins in contrasting lithologic units in the unglaciated and steep terrain of the Oregon Coast Range (Figure 1). This range has an average elevation of 460 m and slopes approaching 50° in many basins (Montgomery, 2001; Roering *et al.*, 2005). This leads to narrow V-shaped valleys highly influenced by moderate to high landslide hazard (Burns, 2017). Long and wet winters produce annually 1500–2000 mm of precipitation received mainly as rainfall (Worona and Whitlock, 1995). The region supports dense forests dominated by Douglas fir (*Pseudotsuga menziesii*).

The dominant geologic formation in the Oregon Coast Range is the Tyee Formation, a rhythmically bedded sandstone deposit. This unit was formed by the deposition of turbidity currents derived from uplifted terrestrial sources (Snavely *et al.*, 1966). Mafic formations from the Middle Eocene to Paleocene intrude sections of the Tyee, producing large outcrops of basaltic composition (Figure 1). These outcrops tend to be more resistant to weathering and erosion than the surrounding sedimentary deposits (O'Connor *et al.*, 2014). The investigated basins were Cummins Creek underlain by basalt (hereafter 'basalt basin') and Green River underlain by sandstone (hereafter 'sandstone basin') (Figure 1). The basalt basin drains 22.0 $km^2$ while the sandstone basin drains 25.6 $km^2$. The basalt basin has a trellis-shaped network, with low-order tributaries directly connected throughout the entirety of the mainstem. The sandstone basin instead has a dendritic network with a major tributary merging with the mainstem 8 km from the headwaters (Figure 1).

Landslides and debris flows are common in the region with historical landslide inventories, showing widespread mass

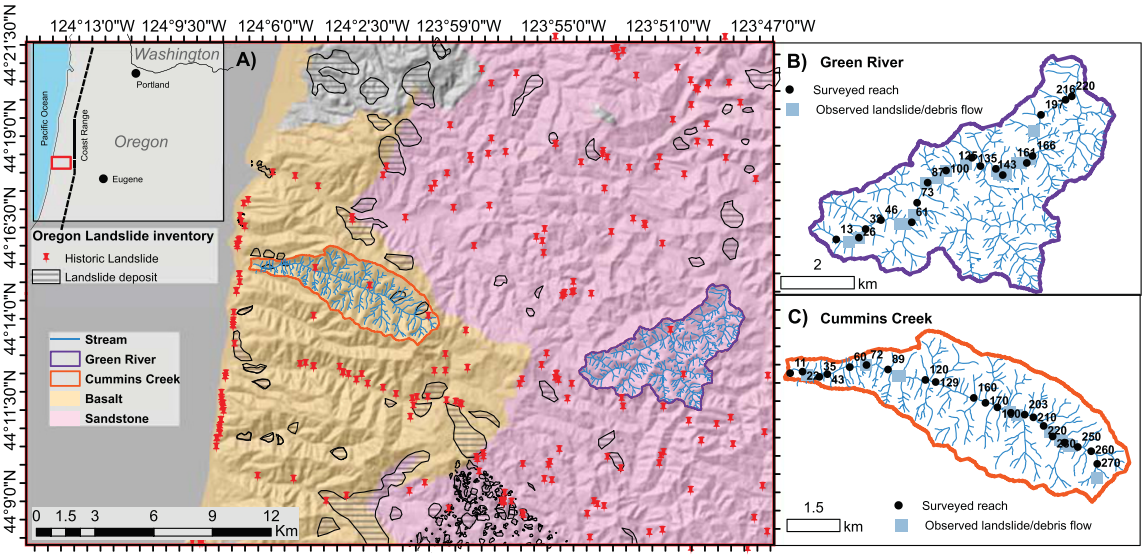


**FIGURE 1.** (A) Dominant lithology (Walker and MacLeod, 1991) and drainage network of the study basins. The map includes historic landslides and landslide deposits from the Oregon Landslide Inventory (Burns, 2017). (B) Surveyed reaches in Green River are underlain by sandstone. (C) Surveyed reaches in Cummins Creek are underlain by basalt. Panels B and C include the location of debris flows and landslides observed in the field (summer 2016). Table S1 in the online Supporting Information includes details of the numbered surveyed reaches in panels B and C [Colour figure can be viewed at wileyonlinelibrary.com]

failures in both sandstone and basalt lithologies. Most recently, the region experienced widespread mass-wasting processes associated with the flood of record in February 1996 when thousands of landslides and debris flows were recorded throughout the Coast (Robinson *et al.*, 1999; May, 2002; Lancaster *et al.*, 2003) and the Cascade (Swanson *et al.*, 1998; Johnson *et al.*, 2000; Miller and Benda, 2000; Faustini and Jones, 2003) ranges. Within the central Coast Range, Lancaster *et al.* (2003) reported a debris flow density of ~7 $km^{-2}$ in a basin underlain by Tyee, 25 km away from the sandstone basin we investigated, while May (2002) estimated a landslide density of 0.4–4.3 $km^{-2}$ that initiated debris flows in 11 basins also underlain by Tyee and located less than 20 km away from the sandstone basin we investigated. Robinson *et al.* (1999) estimated a landslide density of 3.8 $km^{-2}$ across the region, including both sandstone and basalt units. May and Gresswell (2004) found a correlation between valley width and the supply of debris flows sourced from small channel heads considering landslides within the Tyee, with narrow valleys indicating higher connectivity between debris source areas and the mainstem river.

Given the isolated nature of basalt intrusions in the central and southern Coast Range, information on debris flows in basalt basins is limited. Marston *et al.* (1997) investigated debris torrents based on 1978–1979 surveys and concluded that these mass-wasting events were twice as frequent in basalt basins (3.59 debris torrents per 10 km) than in sandstone basins (1.64 debris torrents per 10 km) in a study that included Cummins Creek — the basalt basin investigated here. Robinson *et al.* (1999) reported 4.3 debris flows $km^{-2}$ after the 1996–1997 flood season in basalt basins located 150 km north of Cummins Creek. While no direct assessment of debris flows and landslide events after the 1996 floods was conducted in the investigated basalt or sandstone basins, findings elsewhere suggest that similar processes likely occurred in these basins. Recently, some landslide deposits have been mapped by Oregon Landslide Inventory (Burns, 2017) in the studied basins (Figure 1). Additional evidence for debris flows and landslides was recorded during the field surveys conducted as part of this study (Figures 1B and C).

The study basins are located within a 10 km distance of one another with constant uplift rates over this region (Burgette *et al.*, 2009). Previous erosion rate data indicate regional near topographic equilibrium (Reneau and Dietrich, 1991; Roering *et al.*, 2007) with a long-term erosion rate of ~$1 \times 10^{-4}$ m $year^{-1}$, which is approximately equal to the uplift rate (Kelsey *et al.*, 1994). However, over shorter time scales, the prevalence of stochastic mass-wasting processes has resulted in spatially variable hillslope erosion rates (Heimsath *et al.*, 2001). Normal precipitation (PRISM Climate Group, Oregon State University, http://prism.oregonstate.edu, created 4 Feb 2004) indicates values 20% higher for the basalt basin (2351 mm) than for the sandstone basin (1956 mm).

## Methods

### Channel geometry and grain size

LiDAR and field-collected data were used to determine how channel geometry, grain size, and confinement varied throughout the basins. Drainage areas, elevation, and valley widths were derived from 1-m LiDAR (Oregon Spatial Data Library, https://gis.dogami.oregon.gov/arcgis/rest/services/Public/BareEarth/ImageServer, accessed June 2017) (DOGAMI, 2011) using Topo Toolbox (Schwanghart and Kuhn, 2010). Detailed topographic field surveys of river reaches spaced every 500 m were conducted during the summer of 2016. Twenty-one reaches were surveyed in the basalt basin, and 17 reaches in the sandstone basin (Figure 1, Table S1). All surveyed reaches were relatively straight with few pieces of large wood. Major tributary junctions were 10 channel widths or 40 m away (whichever was greater) from reach locations (Table S1). At each reach an auto-level was used to survey two or three channel cross-sections and a longitudinal profile of the channel bed and water surface elevation over a reach length ~10 times the bankfull width to characterize bankfull channel geometry and channel slope. Bankfull stage was identified by the presence of a break in slope between the channel and the floodplain, as well as considering vegetation and sediment indicators of the transition between the channel and the floodplain (Dunne and Leopold, 1978; Harrelson *et al.*, 1994; Bunte and Abt, 2001). Channel bankfull width was also measured every

~100 m along the mainstems of both rivers with a laser range finder (LTI TruPulse 2011), which resulted in 103–114 width observations in each basin. The estimates of channel width obtained with the laser finder and those calculated from the detailed field topographic channel surveys were not statistically different at the 95% confidence level (*t*-test, *p*-value $> 0.24$). Valley width was estimated in these same locations based on a slope map derived from LiDAR (May *et al.*, 2013). In order to assess potential hillslope coupling (May and Gresswell, 2004), a metric of channel confinement was calculated as the ratio of valley width to bankfull width. Through the field campaign, the entire channel network was visited and the location of landslide and debris flows, evident from the channel, was recorded (Figures 1B and C). Eighteen mass-wasting events were identified in the sandstone and 13 mass-wasting events were identified in the basalt basin.

We characterized the surface grain size distribution (GSD) every 250 m at representative riffles along the mainstem of each basin with 100 pebble counts (Wolman, 1954). This resulted in a total of 40 pebble counts in the basalt basin and 34 pebble counts in the sandstone basin. In addition, the percentage of the channel bed covered in sand was estimated at each of these locations. Subsurface samples were collected every 1000 m over the mainstems at 10 or 11 locations per basin for GSD analysis after removing the surface layer from $> 1$ m$^2$ in exposed sediment bars. In each sample the largest sampled grain was no greater in weight than 5% of the total subsurface sample (Church, 1987). Clasts greater than 32 mm were sieved and weighed in the field, while a subsample of the finer grain size fractions was dry sieved and weighted in a laboratory.

Sternberg's law (Sternberg, 1875) of fining was used to explore longitudinal changes in grain size:

$$W = W_0 e^{(-\alpha x)} \tag{1}$$

where $W_0$ is the initial particle mass, estimated based on the observed $D_{50}$ assuming a constant density per lithology and spherical-shaped grains, $\alpha$ is a loss coefficient, and $x$ is the distance travelled. The potential contribution of abrasion to downstream changes in grain size was investigated using experimentally derived (O'Connor *et al.*, 2014) mass-loss coefficients for sandstone ($\alpha$ = 1.206 km$^{-1}$) and basalt ($\alpha$ = 0.046 km$^{-1}$). O'Connor *et al.* (2014) conducted experiments in which streambed sediments of different lithologies of western Oregon were rotated in a cylinder-shaped tumbler with grain sizes periodically re-measured. Rotations in the tumbler were converted to distance travelled and used to estimate mass-loss coefficients.

### Transport stage and transport capacity

Channel geometry and grain size observations were used to analyse longitudinal trends in sediment transport stage and sediment transport capacity in each river system. Transport stage ($\varphi_{50}$) for the median grain size ($D_{50}$) in the channel bed is defined as the ratio of the bankfull Shields stress ($\tau^*_{50}$) to the critical Shields stress for incipient motion ($\tau^*_{c,50}$):

$$\varphi_{50} = \frac{\tau^*_{50}}{\tau^*_{c,50}} \tag{2}$$

Bankfull shear stress ($\tau$) was calculated assuming uniform flow conditions:

$$\tau = \rho g R S \tag{3}$$

where $\rho$ is water density, $g$ is gravitational acceleration, $R$ is the bankfull hydraulic radius, and $S$ is the water surface slope. Given the difficulty and danger in accessing our sites during winter high-flow conditions, we assumed the water surface slope measured at low-flow conditions is similar to the slope at bankfull flow. The Shields stress ($\tau^*_{50}$) for $D_{50}$ was calculated based on $\tau$:

$$\tau^*_{50} = \frac{\tau}{(\rho_s - \rho) g D_{50}} \tag{4}$$

where $\rho_s$ is the sediment density. A density of 2850 kg m$^{-3}$ was assumed for the basalt basin (Parker *et al.*, 1982) and a density of 2700 kg m$^{-3}$ was assumed for the sandstone basin (Alto, 1981). Given that $\tau^*_c$ varies systematically with slope (Mueller *et al.*, 2005; Lamb *et al.*, 2008), it was estimated using a power-law equation (Pitlick *et al.*, 2008):

$$\tau^*_{c,50} = 0.36 S^{0.46} \tag{5}$$

A surface-based equation (Wilcock and Crowe, 2003) was used to calculate bed load as a metric for sediment transport capacity in units of volume width$^{-1}$ time$^{-1}$ (see the online Supporting Information for equation details). Similar results (not shown) were obtained with other equations (Parker *et al.*, 1982; Recking, 2013).

## Results

### Slope, channel geometry, and grain size

LiDAR-derived channel profiles indicated that the basalt basin drops nearly 650 m in elevation over 15 km compared to a 285 m change in elevation in the sandstone basin over 14 km. Field measurements of slope and LiDAR-derived channel profiles indicated that the basalt basin is systematically steeper, with slopes between 0.008 and 0.14 compared to the sandstone basin with slopes between 0.0019 and 0.08 (Figure 2A). The drainage area of the surveyed reaches across the two basins varied between 0.37 and 25.6 km$^2$. In the context of drainage slope–area plots, drainage areas greater than 0.1 km$^2$ are associated with reaches within the fluvial regime, whereas drainage areas smaller than 0.1 km$^2$ are associated with reaches influenced by hillslope processes such as debris flows, consistent with other basins in the region (May *et al.*, 2013).

In the basalt basin, channel bankfull width varied between 2.6 and 15.1 m (Figure 2B, Table 1). In contrast, in the sandstone basin, bankfull width increased from 2.5 m in the headwaters to around 10.5 m in the lower reaches over 13 km (Figure 2B). Assuming that regionally, discharge scales with drainage area (Castro and Jackson, 2001), power relations between channel geometry and drainage area were estimated. The power relations between drainage area and channel bankfull width were strong in both basins (Table 1). The slope of this relation was higher in the basalt basin than in the sandstone basin, which was in the lower end of observed scaling exponents for most alluvial rivers (Table 1) (Leopold and Maddock, 1953). Valley width increased faster with drainage area than channel width in both systems (Table 1). In the basalt basin, the slope of the drainage area–valley width relation was 1.5 times larger than the slope of the drainage area–channel width relation (Table 1, Figure 2D). In the sandstone basin the slope of the drainage area–valley width relation was twice as large as the slope of the drainage area–channel width relation (Table 1). The drainage area–valley width relations were similar

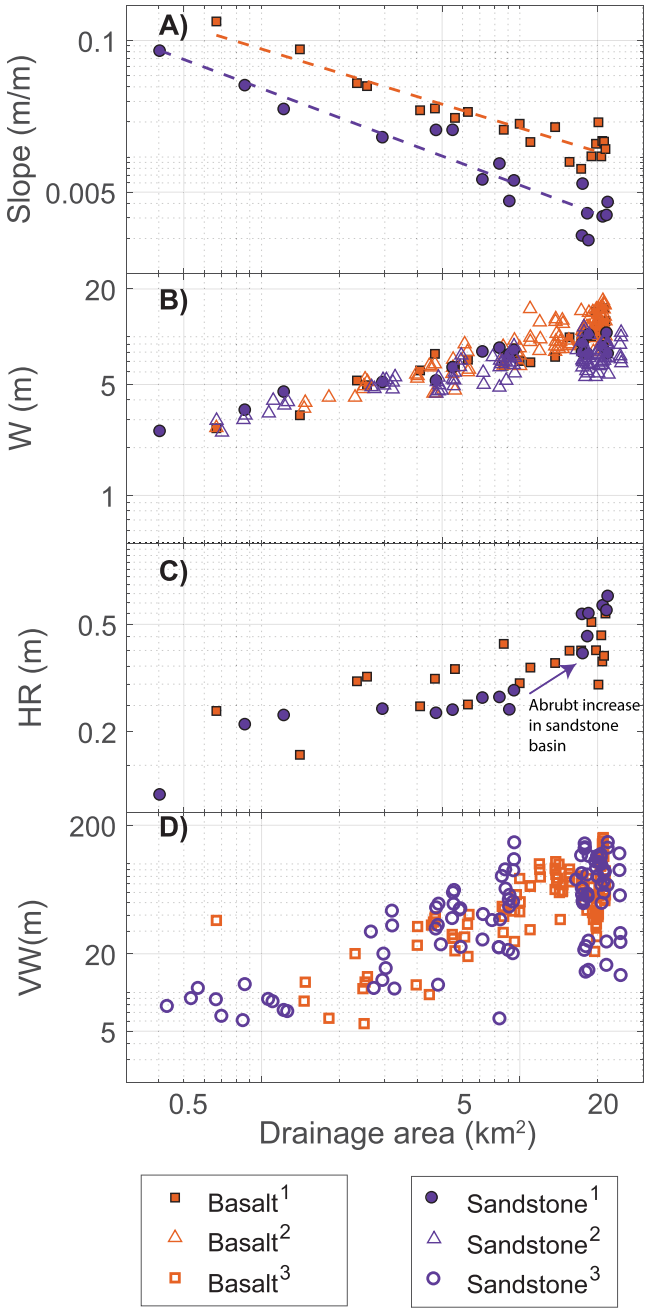


**FIGURE 2.** Drainage area versus channel slope (A), the dashed lines indicate the best-fit power-law relationships; bankfull width, W (B); hydraulic radius, HR (C); and valley width, VW (D). Slope, channel width, and hydraulic radius were measured in the field with detailed topographic surveys (1). Channel width was also measured in the field with a laser range finder (2). Valley width was derived from LiDAR (3) [Colour figure can be viewed at wileyonlinelibrary.com] [Correction added on 27 June 2020 after first online publication: The x axis scale in figure 2 was previously missing and has been updated in this version.]

**Table 1.** Exponents from power-law fits of drainage area (independent variable) versus bankfull channel width and hydraulic radius and valley width (dependent variables). *a* represents the intercept and *b* represents the slope. The values in parentheses are the standard errors of *a* and *b*

| | Basalt | | | | Sandstone | | | |
|---|---|---|---|---|---|---|---|---|
| | Width | | Hydraulic Radius | | Width | | Hydraulic Radius | |
| | *a* | *b* | *a* | *b* | *a* | *b* | *a* | *b* |
| River[†] | 3.73 (0.30) $R^2 = 0.88$ | 0.42 (0.035) | 0.22 (0.02) $R^2 = 0.57$ | 0.21 (0.040) | 3.72 (0.21) $R^2 = 0.91$ | 0.3 (0.025) | 0.17 (0.017) $R^2 = 0.78$ | 0.34 (0.047) |
| Valley[‡] | 10.42 (1.38) $R^2 = 0.57$ | 0.63 (0.052) | | | 10.66 (1.5) $R^2 = 0.52$ | 0.6 (0.058) | | |

[†]From detailed topographic surveys.
[‡]From LiDAR.

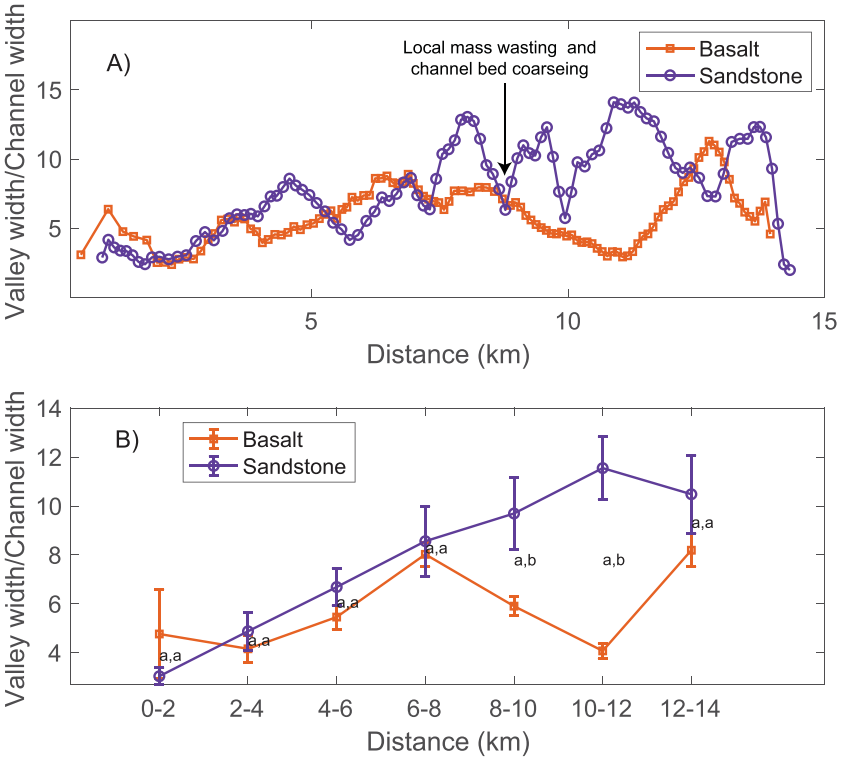


**FIGURE 3.** (A) Confinement (valley width/channel width) in the basalt and sandstone basins. (B) Mean confinement over distance increments. The error bars represent standard errors of the mean. The letters indicate if the difference between confinement in the two basins is significant (student *t*-test). Same letters ('a, a') indicate no statistical difference ($p$-value $> 0.05$) and different letters ('a, b') indicate statistically significant difference ($p$-value $< 0.05$) [Colour figure can be viewed at wileyonlinelibrary.com]

to those derived from LiDAR for sandstone basins in the Oregon Coast Range (May *et al.*, 2013; Beeson *et al.*, 2018).

Channel confinement (i.e., ratio of valley width to channel width) indicated that overall the sandstone basin was less confined than the basalt, implying stronger hillslope influences in the basalt basin (Figure 3A). However, this confinement metric was similar ($t$-test, $p$-value $> 0.5$) and around 5.0 in the two basins for the first 8 km (Figure 3B). Confinement was statistically different between the basalt and sandstone basins between 8 and 12 km (Figure 3B).

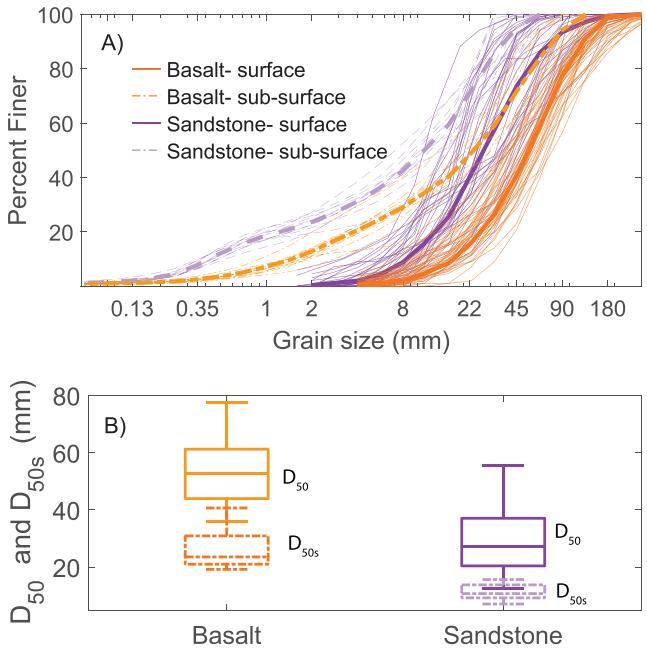


**FIGURE 4.** (A) Comparison of the distributions of surface and subsurface grain sizes for the sandstone and basalt basins in terms of percentage finer and (B) box plots for the distributions of the median grain sizes in the surface ($D_{50}$) and subsurface ($D_{50s}$) across surface pebble counts and subsurface bulk samples. The top and bottom of each 'box' are the 25th and 75th percentiles of the samples, respectively. The distance between the top and bottom corresponds to the interquartile ranges and the line in the middle of each box is the sample median [Colour figure can be viewed at wileyonlinelibrary.com]

Bankfull hydraulic radius in the basalt basin gradually increased from 0.24 m in the headwaters to around 0.55 m in the lower reaches. In the sandstone basin, hydraulic radius varied between 0.12 and 0.63 m, experiencing an abrupt increase (0.28 to 0.54 m) downstream of the confluence of the North and South Forks of Green River at approximately 8 km from the first survey location in the headwaters, where the drainage area increases from 9 to 17 $km^2$ (Figures 2C and S1, Table S1). The drainage area–hydraulic radius relationship was strong in both basins (Table 1). The slope of this relation was smaller for the basalt basin than for the sandstone basin and both slopes were lower than the values reported for other alluvial rivers (Leopold and Maddock, 1953).

Surface and subsurface GSD showed significant variation between and within basins (Figure 4). The basalt basin was coarser (mean $D_{50}$ = 53 mm, mean $D_{84}$ = 114 mm) than the sandstone basin (mean $D_{50}$ = 30 mm, mean $D_{84}$ = 59 mm) (Figure 4). No sand-sized particles were observed in any of the sampled locations except for the last three reaches in the sandstone basin in which sand occupied ~30% of the channel-bed area. Similarly, the subsurface grain sizes in the basalt basin were coarser ($D_{50s}$ = 27 mm, $D_{84s}$ = 66 mm) than in the sandstone basin ($D_{50s}$ = 11 mm, $D_{84s}$ = 33 mm) (Figure 4). However, there is less variability among subsurface samples collected in the sandstone basin than within subsurface samples collected in the basalt basin (Figure 4B).

Longitudinal variability in GSD was remarkably different between the basalt and sandstone basins. However, in the headwater reaches, downstream variations in surface grain size were similar, with both basins displaying $D_{50}$ coarsening (Figure 5). This coarsening trend extended downstream for 5 km in the basalt basin and for 4.5 km in the sandstone basin, with $D_{50}$ increasing in both basins from ~40 to ~55 mm (Figures 5A and B). Over this distance and up to 8 km the two basins had similar confinement (Figure 3). After the initial phase of grain size coarsening, the basalt basin showed no apparent fining trend (Figure 5B). In contrast, the sandstone basin experienced significant downstream grain-size fining between kilometres 4.5 and 8.5 and between kilometres 10 and 13 from the headwaters (Figure 5A). In the first segment, between kilometres 4.5 and 8.5, $D_{50}$ decreased from 55 to 20 mm, potentially because of rapid breakdown of sandstone during transport. A similar decrease was observed for the second segment (kilometres 10–13) with grain size decreasing from 21 to 14 mm. An abrupt local coarsening occurred around kilometres 9–10, matching field observations of sediment inputs from debris flows and landslides (Figure S2). Indeed, 9 out of the 18 mass-movement events observed over the entire surveyed length (Figure 1B) were concentrated between kilometres 8.5 and 9.7 (Figure S2) where the observed coarse surface grain size disrupted the fining trend (Figure 5A). Given that no tributaries entered the mainstem between kilometres 8.5 and 9.7, we inferred that the coarse material observed in these reaches ($D_{50}$ = 35–45 mm) reflects the impact of mass movements. This is also reflected in a decrease in channel confinement at kilometre 9 (Figure 3A). Unlike the sandstone basin, we were unable to link changes in surface grain size in the basalt basin to the presence of debris flow or landslide deposits (Figure S2).

Sternberg's law for fining was applied to explore the longitudinal changes in grain size. The fitted trend for the basalt basin had significant scatter ($r^2$ = 0.1, $p$ = 0.09) and a loss coefficient, $\alpha = -0.063\ km^{-1}$ (Figure 5B). In the sandstone basin, the fitted loss coefficients were similar for the two segments considered (ANCOVA, $p$-value = 0.5) varying between −0.68 and $-0.55\ km^{-1}$. These trends in the sandstone basin were strong, predicting a significant amount ($r^2$ = 0.70–0.74, $p$-value < 0.05) of the overall variation in the measured $D_{50}$. These sandstone loss coefficients were 10 times larger than the loss

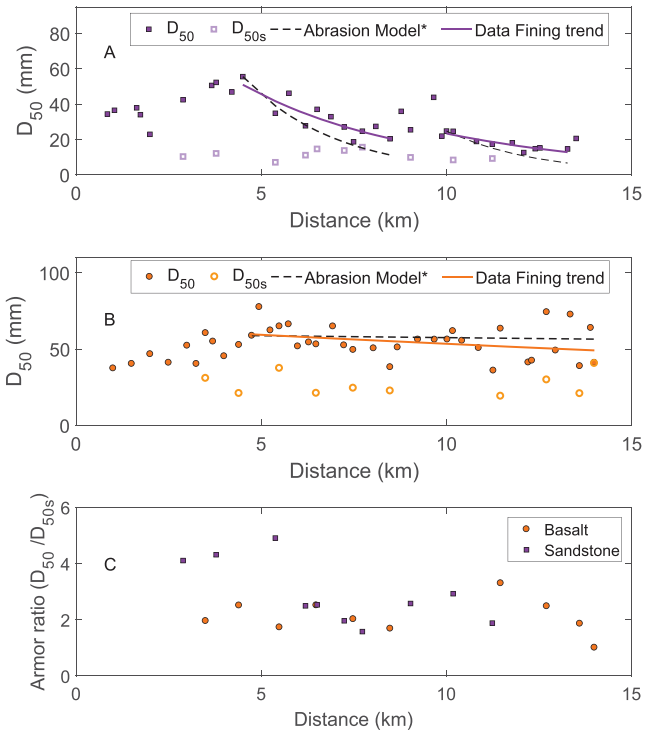


**FIGURE 5.** Downstream changes in the median grain size of the surface ($D_{50}$) and subsurface ($D_{50s}$) in the sandstone (A) and basalt (B) basins and armour ratio ($D_{50}/D_{50s}$) in both basins (C). The solid lines in A and B are the best exponential fit (Equation 1) to the data. The dashed lines in A and B indicate predicted grain sizes based on an abrasion model using calibrated mass-loss coefficients of 0.013 $km^{-1}$ for basalt and 0.1206 $km^{-1}$ for sandstone (O'Connor *et al.*, 2014). In panel A, the observed fining trend in the sandstone basin was divided into two river segments separated by an area of the mainstem that appeared to be heavily impacted by mass wasting (Figure S2 in the online Supplemetary Information) [Colour figure can be viewed at wileyonlinelibrary.com]

coefficients for the basalt basin. Overall, the calculated loss coefficients for the sandstone basin were roughly half the mass-loss coefficients calculated for coastal sedimentary rock ($-1.1206\,km^{-1}$) based on a tumbler experiment (O'Connor *et al.*, 2014).

Despite the mentioned differences in surface grain size patterns, both channel beds were armoured, a feature typical of alluvial gravel-bed rivers (Pitlick *et al.*, 2008). The low variability in subsurface GSD within both basins (Figures 5A and B), combined with the mentioned surface fining trends, resulted in armour ratios ($D_{50}/D_{50s}$) varying between 1 and 3.3 in the basalt basin and between 1.5 and 4.3 in the sandstone basin (Figure 5C).

## Transport stage and transport capacity

Despite lithology-driven differences in grain size, channel geometry, and slope, both basins displayed strong relationships between surface grain size ($D_{50}$ and $D_{84}$) and bankfull shear stress ($\tau$), which reflects the hydraulic sorting of sediment supplied to reaches. In all reaches below the upper river sections in which we observed downstream grain size coarsening (i.e., 5 km in the basalt basin and 4.5 km in the sandstone basin), $\tau$ was strongly correlated ($p < 0.05$) with $D_{50}$ and $D_{84}$ (Figure 6).

The dimensionless Shields stress for the median grain size ($\tau^*_{50}$) represents the ratio of available forces to mobilize sediment to the weight of a given grain size. For drainage areas greater than $2.5\,km^2$, which corresponded to a distance from the headwaters of 2.7 km in the sandstone basin and 2.5 km in the basalt basin, $\tau^*_{50}$ remained relatively constant at approximately 0.045 for both basins (Figure 7A). In all reaches with drainage area less than $2.5\,km^2$, slope had a disproportionate influence in the downstream variation of $\tau^*_{50}$. Slope in both basins changed close to an order of magnitude (0.15 to 0.04 in the basalt basin and 0.08 to 0.03 in the sandstone basin) over these initial few kilometres in contrast to the relatively moderate changes in hydraulic radius and grain size (Figures 2 and 5).

Echoing patterns from the dimensionless Shields stress, transport stage was scattered around a value of 1.1, similar to threshold channels (Parker, 1978, 1979). Exceptions occurred, however, in headwater reaches where transport stages exceeded a value of two before rapidly decreasing to near

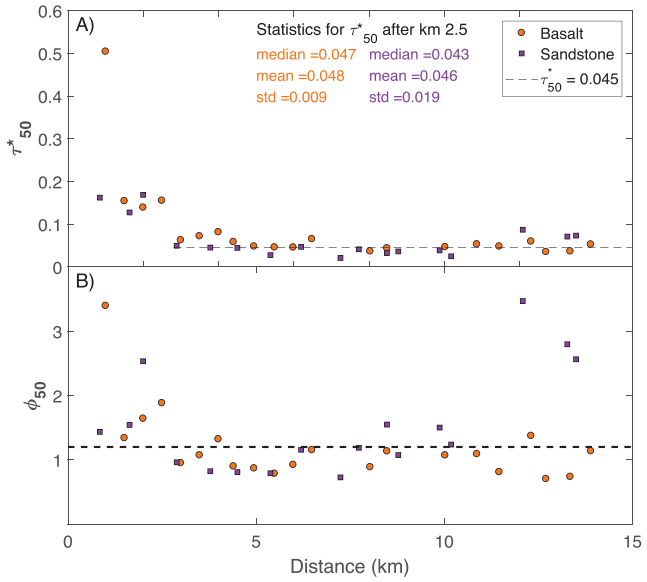


**FIGURE 7.** (A) Dimensionless bankfull Shields stress ($\tau^*_{50}$) as a function of distance downstream; $\tau^*_{50}$ statistics are shown for reaches located >2.5 km from the headwaters in both basins. (B) Downstream trends of transport stage [$\varphi_{50}$, Equation 2)]. The dashed line indicates the $\varphi_{50}$ associated with threshold channels (~1.2) (Parker, 1979) [Colour figure can be viewed at wileyonlinelibrary.com]

threshold values (Figure 7B). These step-pool reaches (Montgomery and Buffington, 1997) were steep with slopes >2%. In the sandstone basin, the last three downstream reaches had transport stages between 2.5 and 3.5 (Figure 7B). These reaches had a high percentage of sand in the bed (~30% of the channel area) and some bedrock outcrops. These observations indicate that these reaches represent a transitional segment from an alluvial to a bedrock channel.

Bankfull sediment transport capacity varied over five orders of magnitude in the basalt basin and over four orders of magnitude in the sandstone basin, decreasing consistently with drainage area in both streams (Figure 8). Although transport capacity trends are similar in both basins, there are one or two orders of magnitude difference at some distances (Figure 8A). The slope of the drainage area–transport capacity relation was higher in the basalt basin than in the sandstone basin (Figure 8). Despite

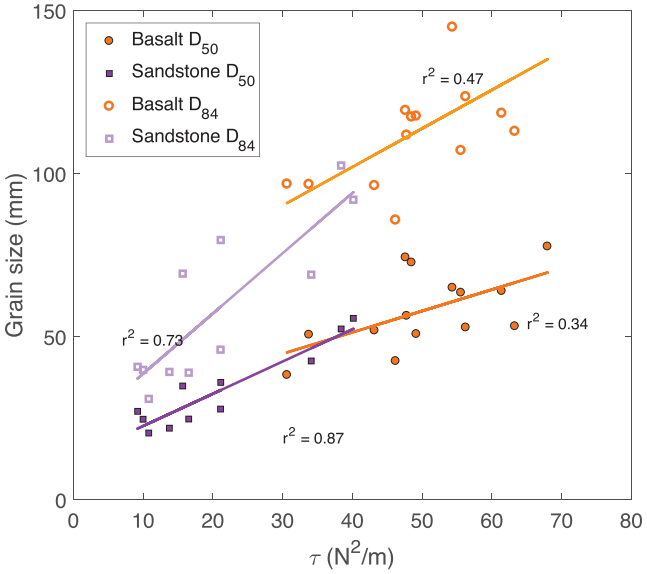


**FIGURE 6.** Scaling of the surface grain size ($D_{50}$ and $D_{84}$) with bankfull shear stress ($\tau$) for all reaches excluding those in which we observed downstream coarsening (upper 5 km in the basalt basin and upper 4.5 km in the sandstone basins). Relationships are significant at the 0.05 level with associated $r^2$ values shown next to the best-fit line [Colour figure can be viewed at wileyonlinelibrary.com]

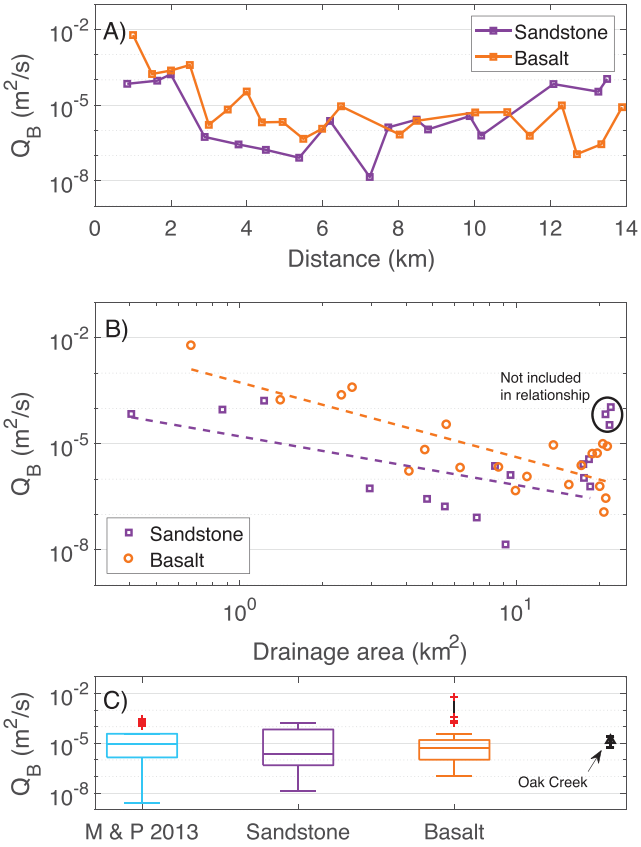


**FIGURE 8.** Variability of volumetric bankfull sediment transport capacity per unit channel width ($Q_B$) with distance (A) and drainage area (B) for the study basins. The dashed lines represent the power fit to the data. The last three reaches in the sandstone basin were not included to derive the power relation. (C) $Q_B$ distributions in the basalt and sandstone basins compared to measured bankfull bed load at 39 mountain streams (Mueller and Pitlick, 2013) and at Oak Creek, OR (Milhous, 1973) [Colour figure can be viewed at wileyonlinelibrary.com]

these differences, mean bankfull transport capacity was similar in both basins (Figure 8) (*t*-test, *p*-value = 0.37). The calculated transport capacity for the last three reaches in the sandstone basin was relatively high, reflecting the effect of the high transport stage (Figure 6). However, the uncertainty in these estimates is higher given that we did not consider the effect of sand content, which is high in these reaches.

The mean estimated bankfull sediment transport capacities in the basalt and sandstone basins were statistically similar (ANOVA, *F*-statistic = 0.51) to bedload in 39 streams in the Northern Rockies (Mueller and Pitlick, 2013) and in Oak Creek, OR (Milhous, 1973) (Figure 8), illustrating that sediment capacity in gravel-bed streams draining hillslope-coupled terrain is similar to transport capacity in other mountain gravel-bed rivers.

## Discussion

Strong evidence of threshold conditions was observed within most of the surveyed length in both study basins. This is contrary to our expectation that the sandstone basin would not display such conditions given high diminution rates in this softer lithology. Cummins Creek, underlain by basalt, had significantly coarser surface and subsurface material and steeper channel slopes compared to Green River, underlain by sandstone. However, in both basins there were strong relationships between shear stress and surface grain size. Although both basins display threshold conditions over at least 60% of their length, we observed lithologically driven differences in the prevalence of this threshold condition, likely controlled by differences in abrasion rates.

### Downstream variation in surface and subsurface grain sizes

The observed downstream coarsening in the headwaters of both basins can be interpreted as evidence for the influence of non-fluvial processes (Brummer and Montgomery, 2003), such as the frequent delivery of coarse grain sizes by mass-movement events (Brummer and Montgomery, 2003; Attal and Lavé, 2006; Attal *et al.*, 2015). This mechanism is likely important in both streams considering that in the headwater reaches of both rivers, valley width is narrow and confinement is similar (Figure 3), indicating that both channels are highly coupled with their hillslopes (May and Gresswell, 2004). Coarsening in the headwaters thus likely reflects the direct contribution of coarse sediment from debris flow and landslide processes. Despite this hillslope influence, the surveyed reaches are located within the fluvial domain, as indicated by the lack of change in the slope of slope–area plots (Figure 2), as opposed to a break distinguishing the transition from the hillslope to the fluvial domain (Montgomery and Foufoula-Georgiou, 1993; Duvall *et al.*, 2004; Wobus *et al.*, 2006). Indeed, such a break has regionally been observed at ~0.1 $km^2$ (May *et al.*, 2013), well below the smallest site considered here (0.41 $km^2$). The slopes of the slope–area plots are similar (0.7–0.8) between the two basins, whereas the intercept for the basalt is double the intercept for the sandstone, highlighting their difference in erodibility (Whipple and

Tucker, 1999). Interestingly, the grain sizes and rates of coarsening were similar in the first few kilometres of both systems (Figures 5A and B), implying that over this distance, where confinement is strong, sediment supply from the hillslope is independent of lithology. Another possible driver of the observed coarsening trend in the headwaters could be associated with variability in the lithology of the supplied sediment, which would result in differential abrasion rates (Mueller *et al.*, 2016). If this were the case, coarse resistant fractions would prevail for longer periods than more friable material in channels with mixed lithology. Given that both Green River and Cummins Creek are primarily underlain by a single lithology, differential abrasion is not likely to be the main physical mechanism to explain the observed coarsening trend.

Although both streams share similar coarsening trends in the headwaters, subsequent downstream fining is significantly different between the two basins and consistent with alluvial abrasion and/or selective transport (Ferguson *et al.*, 1996; O'Connor et al., 2014). Downstream surface fining was evident in the sandstone basin, with fining rates half those predicted based on a tumbler experiment for the same lithologic unit (O'Connor et al., 2014) (Figure 5A). Given that comminution alone could result in even stronger fining trends than those observed, it is likely that in the sandstone basin, selective transport is not an important process. Despite the mechanism (abrasion or selective transport), this trend is in contrast to previous observations in the region that found no distinguishable fining trends in surface grain size of sandstone basins (Marston *et al.*, 1997; Atha, 2013).

In both basins the surface and subsurface grain sizes were sorted into separate layers reflecting a fluvial response to the prevailing hydraulic conditions and sediment supply regime (Parker and Klingeman, 1982; Dietrich *et al.*, 1989; Buffington and Montgomery, 1999; Pfeiffer *et al.*, 2017). The median, $D_{50s}$, in the basalt basin (23.6 mm) was typical of subsurface GSD in many gravel-bed rivers, while the median $D_{50s}$ in the sandstone (10.7 mm) basin fell below the 13th percentile of the subsurface GSD data compiled by Pitlick *et al.* (2008) for Colorado and Idaho, which had a median $D_{50s}$ of 22.8 mm. Similar to other systems, we observed relatively constant subsurface median sizes along the mainstem (Brummer and Montgomery, 2003; Pitlick *et al.*, 2008) that potentially represents the median size of the bed load moving through these reaches (Parker *et al.*, 1982; Dietrich *et al.*, 1989). The armour ratios were similar to other streams in Oregon (O'Connor et al., 2014), Washington (Brummer and Montgomery, 2003), and the Rocky Mountain region (Whiting and King, 2003; Pitlick *et al.*, 2008). Finally, the overall decreasing trend in armoring ratios suggests an overall downstream increase of bed load mobility (Mueller and Pitlick, 2005).

## Shear stress, Shields stress, and transport stage

The strong linear relationships between shear stress and surface grain size fractions suggest downstream adjustments in response to varying hydraulic forces. Increasing trends in $D_{50}$ and $D_{84}$ with shear stress have also been documented in mountain streams in Idaho (Mueller *et al.*, 2016), Colorado (Mueller and Pitlick, 2005), and the Pacific Northwest (Brummer and Montgomery, 2006). These trends are in contrast to recent findings in other mountain streams with contrasting lithology in which finer surface grain sizes were observed for a given shear stress in relatively more friable lithology, reflecting systematically higher Shields stresses and transport rates for friable lithology (Mueller *et al.*, 2016). Mueller *et al.* (2016) argued that higher bed load fluxes resulted in less armoring in the more friable lithology, providing a feedback mechanism whereby bed material can be moved more easily. In our case, the relationship between shear stress and grain size does not appear to depend on lithology. Rather, grain size is a function of a given shear stress across both basins (Figure 6). This is assuming that the relationship shown for the sandstone basin, if continued for larger grain sizes, would follow the same trend as for the basalt basin. The similarity we observed between basalt and sandstone basins implies similar transport rates (Figure 8), with transport stages along both basins clustered around a value of one (Figure 7), suggesting that sediment transport processes maintain threshold channel conditions (Parker, 1979) such that the surface grain size changes consistently with the channel slope and shear stress acting on the bed.

The basalt basin displayed threshold conditions over 80% of the surveyed reaches. In contrast, the sandstone basin, which has high friability, displayed threshold conditions over most of its alluvial extent (i.e., in 60% of surveyed reaches), but deviated from threshold conditions in the last three reaches (Figure 7). In these reaches, the sand-sized fraction was high (~30%), resulting in exposed bedrock outcroppings. We suspect that these reaches mark the transition to a bedrock river. In the steepest headwater reaches — with slopes above 0.05 — transport stage values were greater than one. This could indicate non-threshold conditions or higher uncertainty in the equation used to estimate critical conditions (Pitlick *et al.*, 2008), which was derived for gravel-bed rivers with slopes below 0.05. In the sandstone basin, there appears to be a trade-off between the available sediment and the effects of abrasion with increasing distance downstream. This trade-off was described in part as an alternative state between channel aggradation and channel degradation (Benda, 1990), promoted by the stochastic nature of sediment supply in the region. Our results indicate the spatial extent of threshold-like conditions is strongly lithology dependent.

## Lithology-dependent channel adjustment

In forested mountainous gravel-bed streams the trajectory of adjustment after large sediment pulses appears to depend on channel gradient, channel roughness, the size of the sediment pulse, and the frequency of bed mobilizing flows (Madej, 1999, 2001). Similarly, one-dimensional models and flume experiments demonstrated that following a change in sediment supply, equilibrium transport is re-established through adjustments in surface grain size, roughness, and slope (Dietrich *et al.*, 1989; Buffington and Montgomery, 1999; Eaton and Church, 2009; Madej *et al.*, 2009; Johnson *et al.*, 2015; Müller and Hassan, 2018).

Based on our field observations, we propose a conceptual model to describe lithology-dependent adjustment after the 1996 flood for basalt and sandstone basins (Figure 9). We assumed that both were affected by widespread debris flows after the floods of 1996, similar to other basins in the region (Swanson *et al.*, 1998; Robinson *et al.*, 1999; Johnson *et al.*, 2000; Miller and Benda, 2000; May, 2002; Faustini and Jones, 2003; Lancaster *et al.*, 2003), although it is possible that the basalt basin experienced more events than the sandstone basin (Marston *et al.*, 1997), given that it has steeper tributary junction angles (Miller and Burnett, 2008). In addition, deep-seated landslides in the region are likely to be associated more often with sandstone lithology, influencing channel width through long-term sediment supply (Roering *et al.*, 2005; May *et al.*, 2013; Beeson *et al.*, 2018).

A sporadic sediment input entering basins underlain by basalt would disrupt existing threshold channel conditions for

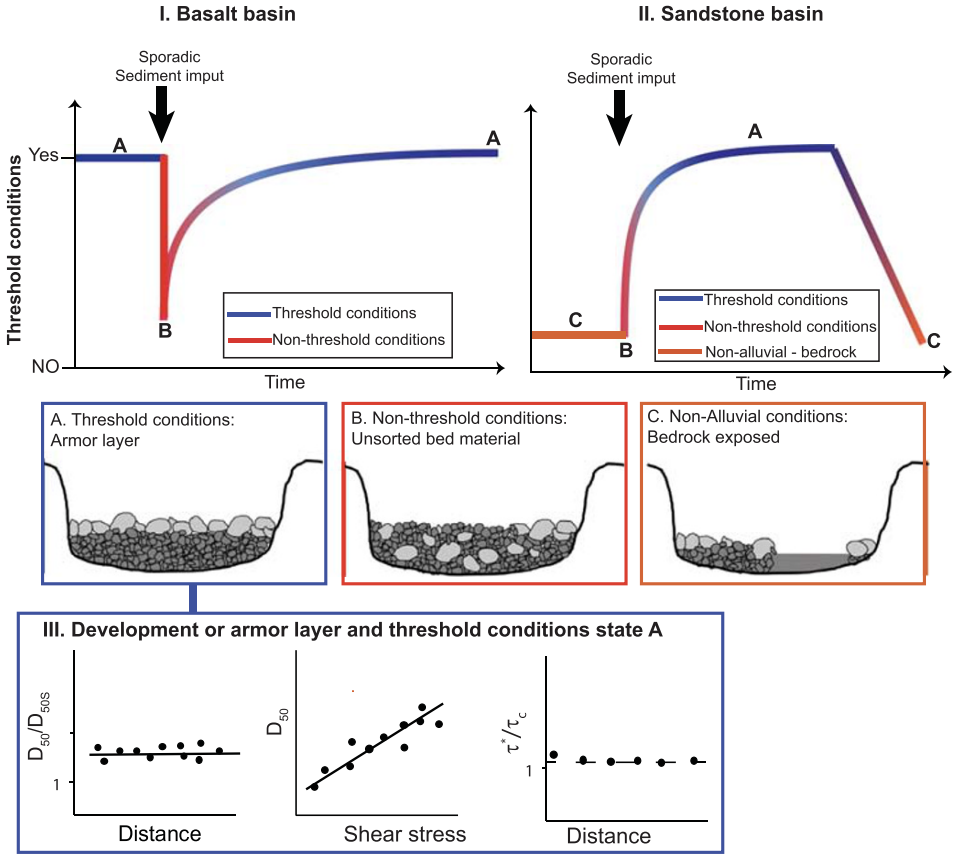


**FIGURE 9.** Conceptual model of the channel bed response and adjustment after a sporadic sediment input from the hillslope. (I) In a river with low abrasion rates, threshold conditions (state A) are disrupted, limiting the ability of the channel to adjust its boundaries for some time and distance (state B). Over time, the sediment supplied is reorganized with little associated loss given the low abrasion rates. Therefore, threshold channel conditions are restored and maintained, presumably until the next significant sediment input occurs. (II) In a river with high abrasion rates, threshold conditions would also evolve (state A). However, the higher abrasion rates could deplete the alluvial material, resulting in non-alluvial conditions with exposed bedrock (state C). The stream with high abrasion could also display threshold conditions (state A) before the sediment input event, if this event occurs before comminution processes deplete the alluvial material. In state A, the bed is armoured while in state B, it is unsorted. State C shows the emergence of a bedrock bed. (III) The characteristics of threshold conditions (state A): armoured bed, strong relation between grain size and shear stress, and bankfull shear stress near the critical for motion. The duration of each state A, B, and C depends on the frequency of mass movement events and on their magnitude [Colour figure can be viewed at wileyonlinelibrary.com]

some time, over which the river could be covered with colluvium and not capable of adjusting its boundaries (Booth and Bledsoe, 2009), temporarily losing its alluvial character (Figure 9). After some time, the channel will rework the bed material and return to threshold-like conditions. This interpretation is consistent with observations in the basalt basin of armoured beds, strong relations between shear stress and grain size, and overall widespread threshold conditions, with the bankfull shear stress near the critical for motion of the median grain sizes. In our conceptual model, the channel bed grain size is the key feature that adjusts rather than the channel size or the slope. That is, the grain size distribution in the channel bed has changed since 1996, while the channel size and slope have likely remained unchanged. This is in agreement with flume (Dietrich *et al*., 1989; Buffington and Montgomery, 1999; Eaton and Church, 2009; Madej *et al*., 2009) and field studies (Mueller and Pitlick, 2013) indicating that channel adjustment to changes in sediment supply occur primarily via the adjustment of the channel grain size.

The sandstone basin could experience an additional state in which bedrock is exposed after all available alluvium is lost to high comminution rates (Figure 9). This is consistent with the strong fining trends observed for the sandstone basin (Figure 5-A), which indicate that abrasion processes could ultimately reduce the available gravel material to sand, limiting the flux of bed load (O'Connor *et al*., 2014). We infer from the observations in the downstream end of the sandstone basin that this system could gradually transition towards a bedrock river until the next major storm triggers large sediment inputs.

Despite uncertainty in how long after the 1996 flooding season streams in the region reached threshold-like conditions, we found evidence that the channels have adjusted to carry the median grain size at bankfull flow. Considering the relatively short time since 1996, it is unlikely that the slope or the channel geometry have changed, implying that adjustment has occurred primarily by sorting and reorganization of the bed material. While it is not possible to know the grain size that the mass movement events delivered during the 1996 floods, our field observations of grain size indicated that the grain size was likely similar between the two basins over the first 4–5 km.

## Conclusion

Longitudinal variations in channel geometry, grain size, and transport capacity were investigated in two basins with contrasting lithology. Despite differences in channel size, slope, and sediment texture, both basins displayed threshold-like conditions with the bankfull shear stress slightly higher than that required to mobilize the median grain size in the channel bed.

The prevalence of threshold conditions was also evident in the vertical sorting of sediment with armoring along both channel networks. While the channel grain size decreased over most of the survey length, it displayed a coarsening trend in the headwater reaches of both systems consistent with strong hillslope influence. We infer a cycle of adjustment to the assumed sediment delivery from the 1996 flooding season, from threshold to non-alluvial to threshold conditions for both lithologies. In addition, the sandstone basin can also experience complete depletion of the alluvium cover leading to bedrock exposure. The prevalence of threshold conditions has lasted since sometime after the last big flood of record in the region in 1996. Thus, our findings suggest that the reaches in the basalt basin will act as threshold channels over longer time frames than the reaches in the sandstone basin. This is despite the fact that debris flows are more frequent in the basalt basin, indicating that the lithologic control on channel adjustment is driven by differences in rock competence that ultimately control grain size fining rates and available gravel for bed load transport.

*Acknowledgements*—We would like to thank Johnathan Tenny for help collecting the field data. This research was funded in part by the National Science Foundation under Grant No. 1619700 and by the USDA National Institute of Food and Agriculture: McIntire Stennis project OREZ-FERM-876. Many thanks to John Pitlick, Erich Mueller, Lee Benda, and Josh Roering for insightful discussions. We thank the Editor Dr. Lane, Dr. Jim Pizzuto, and an anonymous reviewer for their very insightful reviews, which greatly improved this manuscript.

### Data Availability Statement

Cross-sectional data is available in the online Supporting Information. Other data used during the current study are available from the corresponding author on reasonable request.

## Conflict of Interest

The authors have no conflict of interest to declare.

## References

Alto JV. 1981. *Engineering properties of Oregon and Washington coast range soils*. Masters thesis, Oregon State University. Available from Oregon State University ScholarsArchive@OSU database.

Atha JB. 2013. Fluvial wood presence and dynamics over a thirty year interval in forested watersheds. Ph.D. thesis, University of Oregon.

Attal M, Lavé J. 2006. Changes of bedload characteristics along the Marsyandi River (central Nepal): implications for understanding hillslope sediment supply, sediment load evolution along fluvial networks, and denudation in active orogenic belts. *Special Paper 398: Tectonics, Climate, and Landscape Evolution*. Geological Society of America: Boulder, CO.

Attal M, Mudd SM, Hurst MD, Weinman B, Yoo K, Naylor M. 2015. Impact of change in erosion rate and landscape steepness on hillslope and fluvial sediments grain size in the Feather River basin (Sierra Nevada, California). *Earth Surface Dynamics* **3**(1): 201–222. https://doi.org/10.5194/esurf-3-201-2015

Beeson HW, Flitcroft RL, Fonstad MA, Roering JJ. 2018. Deep-seated landslides drive variability in valley width and increase connectivity of salmon habitat in the Oregon Coast Range. *Journal of the American Water Resources Association* **54**(6): 1325–1340. https://doi.org/10.1111/1752-1688.12693

Benda L. 1990. The influence of debris flows on channels and valley floors in the Oregon Coast Range, U.S.A. *Earth Surface Processes and Landforms* **15**(5): 457–466. https://doi.org/10.1002/esp.3290150508

Benda LE, Dunne T. 1987. Sediment routing by debris flow. *Proceedings of International Symposium on Erosion and Sedimentation in the Pacific Rim; IAHS-AISH Publication* **165**: 213–223.

Benda L, Hassan MA, Church M, May CL. 2005. Geomorphology of steepland headwaters: the transition from hillslopes to channels. *Journal of the American Water Resources Association* **41**(4): 835–851.

Booth DB, Bledsoe BP. 2009. Streams and urbanization. In *The Water Environment of Cities*, Baker LA (ed). Springer: Boston, MA; 93–123.

Brardinoni F, Hassan MA, Slaymaker HO. 2003. Complex mass wasting response of drainage basins to forest management in coastal British Columbia. *Geomorphology* **49**(1): 109–124. https://doi.org/10.1016/S0169-555X(02)00166-6

Brummer CJ, Montgomery DR. 2003. Downstream coarsening in headwater channels. *Water Resources Research* **39**(10): WR001981. https://doi.org/10.1029/2003wr001981

Brummer CJ, Montgomery DR. 2006. Influence of coarse lag formation on the mechanics of sediment pulse dispersion in a mountain stream, Squire Creek, North Cascades, Washington, United States. *Water Resources Research* **42**(7): WR004776. https://doi.org/10.1029/2005wr004776

Buffington JM, Montgomery DR. 1999. Effects of sediment supply on surface textures of gravel-bed rivers. *Water Resources Research* **35**(11): 3523, WR900232–3530. https://doi.org/10.1029/1999wr900232

Bunte K, Abt S. 2001. *Sampling Surface and Subsurface Particle-Size Distributions in Wadable Gravel- and Cobble-Bed Streams for Analyses in Sediment Transport, Hydraulics, and Streambed Monitoring*. U. S. Department of Agriculture, Forest Service: Fort Collins, CO.

Burgette RJ, Weldon RJ, II, Schmidt DA. 2009. Interseismic uplift rates for western Oregon and along-strike variation in locking on the Cascadia subduction zone. *Journal of Geophysical Research – Solid Earth* **114**(B1). https://doi.org/10.1029/2008jb005679

Burns W. 2017. Statewide Landslide Information Database for Oregon, Release 3.4. Available at https://www.oregongeology.org/slido/ (accessed 22 March 2019).

Campbell D, Church M. 2003. Reconnaissance sediment budgets for Lynn Valley, British Columbia: Holocene and contemporary time scales. *Canadian Journal of Earth Sciences* **40**(5): 701–713. https://doi.org/10.1139/e03-012

Castro JM, Jackson PL. 2001. Bankfull discharge recurrence intervals and regional hydraulic geometry relationships: patterns in the Pacific Northwest, USA1. *Journal of the American Water Resources Association* **37**(5): 1249–1262. https://doi.org/10.1111/j.1752-1688.2001.tb03636.x

Chatanantavet P, Lajeunesse E, Parker G, Malverti L, Meunier P. 2010. Physically based model of downstream fining in bedrock streams with lateral input. *Water Resources Research* **46**(2): WR007208. https://doi.org/10.1029/2008wr007208

Church M. 1987. River bed gravels: sampling and analysis. *Sediment Transport in Gravel-Bed Rivers* **n/a**: 43–88.

Church M. 2006. Bed material transport and the morphology of alluvial river channels. *Annual Review of Earth and Planetary Sciences* **34**(1): 325–354. https://doi.org/10.1146/annurev.earth.33.092203.122721

Church M. 2010. Mountains and Montane. *Channels* **n/a**: 17–53. https://doi.org/10.1002/9780470682876.ch2

Dietrich W, Kirchner J, Ikeda H, Iseya F. 1989. Sediment supply and the development of the coarse surface layer in gravel-bedded rivers. *Nature* **340**: 215–217. https://doi.org/10.1038/340215a0

DOGAMI. 2011. Oregon Department of Geology and Mineral Industries Lidar Program airborne lidar survey. Available at https://doi.org/10.5069/G9QC01D1 (accessed 1 June 2017).

Dunne T, Leopold LB. 1978. *Water in Environmental Planning*. W. H. Freeman: San Francisco, CA.

Duvall A, Kirby E, Burbank D. 2004. Tectonic and lithologic controls on bedrock channel profiles and processes in coastal California. *Journal of Geophysical Research – Earth Surface* **109**(F3): F000086. https://doi.org/10.1029/2003jf000086

Eaton BC, Church M. 2007. Predicting downstream hydraulic geometry: a test of rational regime theory. *Journal of Geophysical Research – Earth Surface* **112**(F3): F000734. https://doi.org/10.1029/2006jf000734

Eaton BC, Church M. 2009. Channel stability in bed load-dominated streams with nonerodible banks: inferences from experiments in a sinuous flume. *Journal of Geophysical Research – Earth Surface* **114** (F1): F000902. https://doi.org/10.1029/2007jf000902

Eaton B, Millar R. 2017. Predicting gravel bed river response to environmental change: the strengths and limitations of a regime-based approach. *Earth Surface Processes and Landforms* **42**(6): 994–1008. https://doi.org/10.1002/esp.4058

Faustini JM, Jones JA. 2003. Influence of large woody debris on channel morphology and dynamics in steep, boulder-rich mountain streams, western Cascades, Oregon. *Geomorphology* **51**(1–3): 187–205. https://doi.org/10.1016/s0169-555x(02)00336-7

Ferguson R, Hoey T, Wathen S, Werritty A. 1996. Field evidence for rapid downstream fining of river gravels through selective transport. *Geology* **24**(2): 179–182. https://doi.org/10.1130/0091-7613(1996)024<0179:fefrdf>2.3.co;2

Green K, Alila Y, Brardinoni F. 2015. Patterns of bedload entrainment and transport in forested headwater streams of the Columbia Mountains, Canada. *Earth Surface Processes and Landforms* **40**(4): 427–446. https://doi.org/10.1002/esp.3642

Harrelson C, Rawlins C, Potyondy J. 1994. *Stream channel reference sites: an illustrated guide to field technique*. General Technical Report RM-245, U.S. Department of Agriculture, Forest Service, Fort Collins, CO.

Heimsath A, Dietrich W, Nishiizumi K, Finkel R. 2001. Stochastic processes of soil production and transport: erosion rates, topographic variation and cosmogenic nuclides in the Oregon coast range. *Earth Surface Processes and Landforms* **26**: 531–552. https://doi.org/10.1002/esp.209

Johnson JPL, Aronovitz AC, Kim W. 2015. Coarser and rougher: effects of fine gravel pulses on experimental step-pool channel morphodynamics. *Geophysical Research Letters* **42**(20): 8432–8440. https://doi.org/10.1002/2015GL066097

Johnson JPL, Whipple KX, Sklar LS, Hanks TC. 2009. Transport slopes, sediment cover, and bedrock channel incision in the Henry Mountains, Utah. *Journal of Geophysical Research – Earth Surface* **114** (F2): F000862. https://doi.org/10.1029/2007jf000862

Johnson SL, Swanson FJ, Grant GE, Wondzell SM. 2000. Riparian forest disturbances by a mountain flood — the influence of floated wood. *Hydrological Processes* **14**(16–17): 3031–3050. https://doi.org/10.1002/1099-1085(200011/12)14:16/17<3031::AID-HYP133>3.0.CO;2-6

Johnstone SA, Hilley GE. 2015. Lithologic control on the form of soil-mantled hillslopes. *Geology* **43**(1): 83–86. https://doi.org/10.1130/g36052.1

Jones JA, Swanson FJ, Wemple BC, Snyder KU. 2000. Effects of roads on hydrology, geomorphology, and disturbance patches in stream networks. *Conservation Biology* **14**(1): 76–85. https://doi.org/10.1046/j.1523-1739.2000.99083.x

Kelsey HM, Engebretson DC, Mitchell CE, Ticknor RL. 1994. Topographic form of the coast ranges of the Cascadia Margin in relation to coastal uplift rates and plate subduction. *Journal of Geophysical Research – Solid Earth* **99**(B6): 12245–12255. https://doi.org/10.1029/93jb03236

Korup O. 2004. Landslide-induced river channel avulsions in mountain catchments of southwest New Zealand. *Geomorphology* **63**(1–2): 57–80. https://doi.org/10.1016/j.geomorph.2004.03.005

Kuo CW, Brierley G. 2014. The influence of landscape connectivity and landslide dynamics upon channel adjustments and sediment flux in the Liwu Basin, Taiwan. *Earth Surface Processes and Landforms* **39** (15): 2038–2055. https://doi.org/10.1002/esp.3598

Lamb MP, Dietrich WE, Venditti JG. 2008. Is the critical Shields stress for incipient sediment motion dependent on channel-bed slope? *Journal of Geophysical Research – Earth Surface* **113**: F000831. https://doi.org/10.1029/2007jf000831

Lancaster ST, Hayes SK, Grant GE. 2003. Effects of wood on debris flow runout in small mountain watersheds. *Water Resources Research* **39** (6): WR001227. https://doi.org/10.1029/2001wr001227

Leopold L, Maddock T. 1953. *The hydraulic geometry of stream channels and some physiographic implications*. Geological Survey Professional Paper 252.

Madej MA. 1999. Temporal and spatial variability in thalweg profiles of a gravel-bed river. *Earth Surface Processes and Landforms* **24**(12): 1153–1169. https://doi.org/10.1002/(SICI)1096-9837(199911)24:12<1153::AID-ESP41>3.0.CO;2-8

Madej MA. 2001. Development of channel organization and roughness following sediment pulses in single-thread, gravel bed rivers. *Water Resources Research* **37**(8): 2259–2272. https://doi.org/10.1029/2001wr000229

Madej MA, Sutherland DG, Lisle TE, Pryor B. 2009. Channel responses to varying sediment input: a flume experiment modeled after Redwood Creek, California. *Geomorphology* **103**(4): 507–519. https://doi.org/10.1016/j.geomorph.2008.07.017

Marston RA, Fritz DE, Nordberg V. 1997. The impact of debris torrents on substrates of mountain streams. *Géomorphologie: relief, processus, environnement* **3**: 21–32. https://doi.org/10.3406/morfo.1997.898

Massong T, Montgomery D. 2000. Influence of sediment supply, lithology, and wood debris on the distribution of bedrock and alluvial channels. *Bulletin of the Geological Society of America* **112**: 591–599. https://doi.org/10.1130/0016-7606(2000)112<591:IOSSLA>2.0.CO;2

May CL. 2002. Debris flows through different forest age classes in the central Oregon Coast Range1. *Journal of the American Water Resources Association* **38**(4): 1097–1113. https://doi.org/10.1111/j.1752-1688.2002.tb05549.x

May CL, Gresswell RE. 2003. Large wood recruitment and redistribution in headwater streams in the southern Oregon Coast Range, USA. *Canadian Journal of Forest Research-Revue Canadienne De Recherche Forestiere* **33**(8): 1352–1362. https://doi.org/10.1139/x03-023

May CL, Gresswell RE. 2004. Spatial and temporal patterns of debris-flow deposition in the Oregon Coast Range, USA. *Geomorphology* **57**(3): 135–149. https://doi.org/10.1016/S0169-555X(03)00086-2

May C, Roering J, Eaton LS, Burnett KM. 2013. Controls on valley width in mountainous landscapes: the role of landsliding and implications for salmonid habitat. *Geology* **41**(4): 503–506. https://doi.org/10.1130/g33979.1

Menting F, Langston AL, Temme AJAM. 2015. Downstream fining, selective transport, and hillslope influence on channel bed sediment in mountain streams, Colorado Front Range, USA. *Geomorphology* **239**: 91–105. https://doi.org/10.1016/j.geomorph.2015.03.018

Milhous R. 1973. *Sediment transport in a gravel bottomed stream*. Ph.D. thesis, Oregon State University.

Miller DJ, Benda LE. 2000. Effects of punctuated sediment supply on valley-floor landforms and sediment transport. *Geological Society of America Bulletin* **112**(12): 1814–1824. https://doi.org/10.1130/0016-7606(2000)112<1814:eopsso>2.0.co;2

Miller DJ, Burnett KM. 2008. A probabilistic model of debris-flow delivery to stream channels, demonstrated for the Coast Range of Oregon, USA. *Geomorphology* **94**(1–2): 184–205. https://doi.org/10.1016/j.geomorph.2007.05.009

Montgomery D. 2001. Slope distributions, threshold hillslopes, and steady-state topography. *American Journal of Science* **301**: 432–454. https://doi.org/10.2475/ajs.301.4-5.432

Montgomery DR, Buffington JM. 1997. Channel-reach morphology in mountain drainage basins. *Geological Society of America Bulletin* **109**(5): 596–611. https://doi.org/10.1130/0016-7606(1997)109<0596:crmimd>2.3.co;2

Montgomery DR, Foufoula-Georgiou E. 1993. Channel network source representation using digital elevation models. *Water Resources Research* **29**(12): 3925–3934. https://doi.org/10.1029/93wr02463

Montgomery DR, Massong TM, Hawley SCS. 2003. Influence of debris flows and log jams on the location of pools and alluvial channel reaches, Oregon Coast Range. *Bulletin of the Geological Society of America* **115**: 78–88. https://doi.org/10.1130/0016-7606(2003)115<0078:IODFAL>2.0.CO;2

Mouri G, Shiiba M, Hori T, Oki T. 2011. Modeling shallow landslides and river bed variation associated with extreme rainfall-runoff events in a granitoid mountainous forested catchment in Japan. *Geomorphology* **125**(2): 282–292. https://doi.org/10.1016/j.geomorph.2010.10.008

Mueller ER, Pitlick J. 2005. Morphologically based model of bed load transport capacity in a headwater stream. *Journal of Geophysical*

*Research – Earth Surface* **110**: F000117. https://doi.org/10.1029/2003jf000117

Mueller ER, Pitlick J. 2013. Sediment supply and channel morphology in mountain river systems: 1. Relative importance of lithology, topography, and climate. *Journal of Geophysical Research – Earth Surface* **118**(4): 2325–2342. https://doi.org/10.1002/2013jf002843

Mueller ER, Pitlick J. 2014. Sediment supply and channel morphology in mountain river systems: 2. Single thread to braided transitions. *Journal of Geophysical Research – Earth Surface* **119**(7): 1516–1541. https://doi.org/10.1002/2013jf003045

Mueller ER, Pitlick J, Nelson JM. 2005. Variation in the reference shields stress for bed load transport in gravel-bed streams and rivers. *Water Resources Research* **41**(4): WR003692. https://doi.org/10.1029/2004wr003692

Mueller ER, Smith ME, Pitlick J. 2016. Lithology-controlled evolution of stream bed sediment and basin-scale sediment yields in adjacent mountain watersheds, Idaho, USA. *Earth Surface Processes and Landforms* **41**: 1869–1883. https://doi.org/10.1002/esp.3955

Müller T, Hassan MA. 2018. Fluvial response to changes in the magnitude and frequency of sediment supply in a 1-D model. *Earth Surface Dynamics* **6**(4): 1041–1057. https://doi.org/10.5194/esurf-6-1041-2018

Nakamura F, Swanson FJ. 1993. Effects of coarse woody debris on morphology and sediment storage of a mountain stream system in Western Oregon. *Earth Surface Processes and Landforms* **18**(1): 43–61. https://doi.org/10.1002/esp.3290180104

O'Connor JE, Mangano JF, Anderson SW, Wallick JR, Jones KL, Keith MK. 2014. Geologic and physiographic controls on bed-material yield, transport, and channel morphology for alluvial and bedrock rivers, western Oregon. *Geological Society of America Bulletin* **126** (3–4): 377–397. https://doi.org/10.1130/b30831.1

Parker G. 1978. Self-formed straight rivers with equilibrium banks and mobile bed 2. Gravel river. *Journal of Fluid Mechanics* **89**: 127.

Parker G. 1979. Hydraulic geometry of active gravel rivers. *Journal of the Hydraulics Division, ASCE* **105**: 1185–1201.

Parker G, Klingeman PC. 1982. On why gravel bed streams are paved. *Water Resources Research* **18**(5): 1409–1423. https://doi.org/10.1029/WR018i005p01409

Parker G, Klingeman PC, McLean DG. 1982. Bedload and size distribution in paved gravel-bed streams. *Journal of the Hydraulics Division, ASCE* **108**: 544–571.

Parker G, Wilcock PR, Paola C, Dietrich WE, Pitlick J. 2007. Physical basis for quasi-universal relations describing bankfull hydraulic geometry of single-thread gravel bed rivers. *Journal of Geophysical Research – Earth Surface* **112**(F4): F000549. https://doi.org/10.1029/2006jf000549

Pfeiffer AM, Finnegan NJ, Willenbring JK. 2017. Sediment supply controls equilibrium channel geometry in gravel rivers. *Proceedings of the National Academy of Sciences* **114**(13): 3346–3351. https://doi.org/10.1073/pnas.1612907114

Pitlick J, Cress R. 2002. Downstream changes in the channel geometry of a large gravel bed river. *Water Resources Research* **38**: 1–34.

Pitlick J, Mueller ER, Segura C, Cress R, Torizzo M. 2008. Relation between flow, surface-layer armoring and sediment transport in gravel-bed rivers. *Earth Surface Processes and Landforms* **33**(8): 1192–1209. https://doi.org/10.1002/esp.1607

Pizzuto JE. 1992. The morphology of graded gravel rivers: a network perspective. *Geomorphology* **5**: 457–474. https://doi.org/10.1016/0169-555X(92)90018-J

Pizzuto JE. 1995. Downstream fining in a network of gravel-bedded rivers. *Water Resources Research* **31**(3): 753–759. https://doi.org/10.1029/94wr02532

Recking A. 2013. Simple method for calculating reach-averaged bedload transport. *Journal of Hydraulic Engineering* **139**: 70–75. https://doi.org/10.1061/(ASCE)HY.1943-7900.0000653

Reid SC, Lane SN, Berney JM, Holden J. 2007. The timing and magnitude of coarse sediment transport events within an upland, temperate gravel-bed river. *Geomorphology* **83**(1): 152–182. https://doi.org/10.1016/j.geomorph.2006.06.030

Reneau S, Dietrich W. 1991. Erosion rates in the southern oregon coast range: evidence for an equilibrium between hillslope erosion and sediment yield. *Earth Surface Processes and Landforms* **16**: 307–322. https://doi.org/10.1002/esp.3290160405

Richardson JS, Sidle RC, Gomi T. 2002. Understanding processes and downstream linkages of headwater systems: headwaters differ from downstream reaches by their close coupling to hillslope processes, more temporal and spatial variation, and their need for different means of protection from land use. *Bioscience* **52**(10): 905–916. https://doi.org/10.1641/0006-3568(2002)052[0905:upadlo]2.0.co;2

Rickenmann D, Koschni A. 2010. Sediment loads due to fluvial transport and debris flows during the 2005 flood events in Switzerland. *Hydrological Processes* **24**(8): 993–1007. https://doi.org/10.1002/hyp.7536

Robinson EG, Mills K, Paul J, Dent L, Skaugset AE. 1999. Storm impacts and landslides of 1996: Final report. Available at https://people.wou.edu/~taylors/g407/robison_etal_1999.pdf.

Roering JJ, Kirchner JW, Dietrich WE. 2005. Characterizing structural and lithologic controls on deep-seated landsliding: implications for topographic relief and landscape evolution in the Oregon Coast Range, USA. *Geological Society of America Bulletin* **117**: 654. https://doi.org/10.1130/B25567.1

Roering J, Perron T, Kirchner J. 2007. Functional relationships between denudation and hillslope form and relief. *Earth and Planetary Science Letters* **264**: 245–258. https://doi.org/10.1016/j.epsl.2007.09.035

Sable KA, Wohl E. 2006. The relationship of lithology and watershed characteristics to fine sediment deposition in streams of the Oregon Coast Range. *Environmental Management* **37**: 659–670. https://doi.org/10.1007/s00267-005-0055-z

Schwanghart W, Kuhn NJ. 2010. TopoToolbox: a set of Matlab functions for topographic analysis. *Environmental Modelling & Software* **25**(6): 770–781. https://doi.org/10.1016/j.envsoft.2009.12.002

Slaymaker O. 1993. The sediment budget of the Lillooet River Basin, British Columbia. *Physical Geography* **14**(3): 304–320. https://doi.org/10.1080/02723646.1993.10642482

Snavely P, Wagner H, MacLeod N. 1966. *Rhythmic-bedded Eugeosynclinal Deposits of the Tyee Formation, Oregon Coast Range*, Vol. **2**. Kansas Geological Survey: Lawrence, KS.

Sternberg H. 1875. Untersuchungen über längen- und querprofil geschiebeführender flüss. *Zeitschrift für Bauwesen* **11**(12): 483–506.

Swanson FJ, Fredriksen RL, McCorison FM. 1982. *Material Transfer in a Western Oregon Forested Watershed: Stroudsburg*. distributed worldwide by Academic Press: Pa. : Hutchinson Ross Pub. Co.; [New York].

Swanson FJ, Johnson SL, Gregory SV, Acker SA. 1998. Flood disturbance in a forested mountain landscape: interactions of land use and floods. *Bioscience* **48**(9): 681–689. https://doi.org/10.2307/1313331

Torizzo M, Pitlick J. 2004. Magnitude-frequency of bed load transport in mountain streams in Colorado. *Journal of Hydrology* **290**(1–2). https://doi.org/10.1016/j.hydrol.2003.12.001

Tranel LM. 2018. Hillslope coupled stream morphology, flow conditions, and their effects on detrital sedimentology in Garnet Canyon, Teton Range, Wyoming. *Geoscience Frontiers* **9**(4): 1193–1202. https://doi.org/10.1016/j.gsf.2017.07.005

Walker GW, MacLeod NS (Cartographer). 1991. Geologic map of Oregon: scale 1:500,000, 2 sheets. U.S. Geological Survey.

Wells SG, Harvey AM. 1987. Sedimentologic and geomorphic variations in storm-generated alluvial fans, Howgill Fells, northwest England. *GSA Bulletin* **98**(2): 182–198. https://doi.org/10.1130/0016-7606(1987)98<182:sagvis>2.0.co;2

Whipple KX, Tucker GE. 1999. Dynamics of the stream-power river incision model: implications for height limits of mountain ranges, landscape response timescales, and research needs. *Journal of Geophysical Research – Solid Earth* **104**(B8): 17661–17674. https://doi.org/10.1029/1999jb900120

Whiting PJ, King JG. 2003. Surface particle sizes on armoured gravel streambeds: effects of supply and hydraulics. *Earth Surface Processes and Landforms* **28**(13): 1459–1471. https://doi.org/10.1002/esp.1049

Wilcock PR, Crowe JC. 2003. Surface-based transport model for mixed-size sediment. *Journal of Hydraulic Engineering, ASCE* **129**: 120–128.

Wobus C, Whipple KX, Kirby E, Snyder N, Johnson J, Spyropolou K, Crosby B, Sheehan D. 2006. Tectonics from topography: procedures, promise, and pitfalls. In, Willett SD, Hovius N, Brandon MT, Fisher

DM (Eds), Tectonics, Climate, and Landscape Evolution (Vol. **398**. Geological Society of America: Boulder, CO.

Wolman G. 1954. A method of sampling coarse river-bed material. *Eos, Transactions of the American Geophysical Union* **35**(6): 951–956. https://doi.org/10.1029/TR035i006p00951

Worona M, Whitlock C. 1995. Late Quaternary vegetation and climate history near Little Lake, central Coast Range, Oregon. *Geological Society of America Bulletin* **107**: 867–876. https://doi.org/10.1130/0016-7606(1995)107<0867:LQVACH>2.3.CO;2

## Supporting Information

Additional supporting information may be found online in the Supporting Information section at the end of the article.

**Figure S1.** Distance from the headwaters versus bankfull width, W (A); hydraulic radius, HR (B); and valley width, VW (C). Channel width and hydraulic radius were measured in the field with detailed topographic surveys (1). Channel width was also measured in the field with a laser range (2). Valley width was derived from LiDAR (3).

**Figure S2A**. Surface grain size in the basalt basins along with the location of debris flows and landslides observed during the field campaign in 2016. Details of one debris flow is provided in the red square as an example.

**Figure S2B.** Surface grain size in the sandstone basin along with the location of debris flows and landslides observed during the field campaign in 2016. Details of the river section in which coarsening was observed are provided in the red square.

**Table S1.** Location and geomorphic characteristics of the surveyed reaches in Green River and Cummins Creek